Supporting Information

Revolutionizing the Capture Efficiency of Ultrasensitive Digital ELISA via Antibody Oriented-Immobilization Strategy

Yutong Zhang, Xiaojun Kuang, Jingwei Yi, Tong Sun, Qingsheng Guo, Hongchen Gu, Hong Xu*

School of Biomedical Engineering, Med-X Research Institute, Shanghai Jiao Tong University, Shanghai 200030, China

* Corresponding authors.
E-mails: xuhong@sjtu.edu.cn (Hong Xu)

1. Analysis of the k_{on} improvement of CEA-Ab@BA@MBs compared with CEA-Ab@MBs

First, the actual antibody concentrations of CEA-Ab@BA@MBs and CEA-Ab@MBs were acquired by BCA protein quantification. The effective antibody population on CEA-Ab@BA@MBs at 15 μg/mg was 8.5×10^{-10} mol/L on the assumption that all oriented antibodies were functional. As the $F(ab')_2$ fragment amount of CEA-Ab@BA@MBs was 1.65 times higher than CEA-Ab@MBs, the concentration of usable antibody of CEA-Ab@MBs was calculated as 5.1×10^{-10} mol/L, 39.4% of the which are functionless compare to CEA-Ab@BA@MBs.

Second, the concentrations of immunocomplex captured by CEA-Ab@MBs at 1800 s under different k_{on} and k_{off}, determined as [CapAb+Ag], were calculated according to the differential equations (Eq. (1)). The differential equation for the homogeneous reaction of antigens and antibodies (Eq. (1)) was as follows:

$$d[X]/dt = k_{on}\left([Ag_0] - [X]\right)\left([Ab_0] - [X]\right) - k_{off}[X] \quad (1)$$

$[X]$ meant the concentration of immunocomplex generated until "t" moment. $[Ag_0]$ referred to the concentration of antigen fed in the reaction system, which was 8.3×10^{-14} mol/L when λ was 10. $[Ab_0]$ referred to the antibody concentration at the beginning of the reaction, which was 5.1×10^{-10} mol/L when the CEA-Ab@MBs was 15 μg/mg. The specific k_{on} and k_{off} values of CEA-Ab@MBs were named as k_{on1} and k_{off1}. At the same reaction condition, the immunocomplex concentration formed by CEA-Ab@BA@MBs was regarded as [CapAb+Ag]', and the binding rate constant of CEA-Ab@BA@MBs was determined as k_{on2}. Since the capture efficiency of the CEA-Ab@BA@MBs at 1800 s was found to be 14 times greater than that of the CEA-Ab@MBs (Figure 4(e)) according to the experiment result, [CapAb+Ag]' was equal to 14×[CapAb+Ag]. Table S4 showed the values of [CapAb+Ag] under different k_{on1} and k_{off1} and corresponding [CapAb+Ag]'.

Third, the relationship between k_{on2} and [CapAb+Ag]' was fitted on the premise of 8.5×10^{-10} mol/L antibody concentration and typical k_{off} values of antibody in ELISA bioassay, as depicted in Figure S4. After that, a series of [CapAb+Ag]' calculated before were taken as the ordinate of the fitting curve to determine the corresponding k_{on2}, which represented the actual binding rate constant of CEA-Ab@BA@MBs. The values of k_{on1}, k_{on2}, and k_{on2}/k_{on1} were summarized and presented in Table 1.

2. Analysis of the k_{on} improvement of CEA-Ab@MBs with the increase in antibody density

In our previous assumption, the density of randomly coupled antibodies only affected the total bound antigen number rather than the binding ability of every antibody in bead-based digital ELISA. The relationship between the concentration of bound species with the concentration of antibody in an equilibrium state in the homogeneous immunoreaction was stimulated as below:

When the immunoreaction reached equilibrium, $d[X]/dt = 0$, so the equation could be simplified as:

$$k_{on}\left([Ag_0] - [X]\right)\left([Ab_0] - [X]\right) - k_{off}[X] = 0 \quad (2)$$

And Eq. (2) could be transformed as Eq. (3):

$$y = A(B - y)(x - y) \quad (3)$$

where A represents K_D, B is the antigen fed in the reaction system, y is defined as the concentration of the bound species, and x is defined as antibody concentration. After taking the derivative of x on both sides of this equation, it changed to Eq. (4):

$$dy/dx = (B - y)/(1/A + B + x - y) \quad (4)$$

The change of bound species concentration with antibody concentration under different K_D could be clarified by solving this nonrigid differential equations in MATLAB. Afterwards, we divided the concentration of bound species by antibody concentration to obtain the average bound species concentration per antibody. As shown in Figure S5, the higher the antibody content led to the lower the capture efficiency unit antibody in the homogeneous reaction because the concentration of maximal immunocomplex gradually reached saturation with the increase of antibody amounts. However, the experiment results of the Figure 4(g) clearly showed that, in practice, the relative capture efficiency of CEA-Ab@MBs increased with the surge of antibody content no matter how long the incubation took, which made us deny our previous assumption and propose new thesis that the performance of the antibody on the solid phase carrier surface changed with the increase of antibody density. As the rate of chemical reaction not only be affected by the concentration of reactants and products but also depends on the reaction rate constant, we considered the antibody-antigen complex will be formed faster under higher k_{on} when the reactant concentration and k_{off} remain unchanged, so the capture efficiency of each antibody in the non-equilibrium state was significantly improved. In other aspects, we have proposed the antibody conformation model where the denser arrangement of antibodies gave rise to a more consistent orientation. Accordingly, at this stage of understanding, we believed it was well justified that the improvement of k_{on} accelerated antigen binding as the amount of randomly immobilized antibody increased on the surface of CEA-Ab@MBs. Under this hypothesis, the phenomenon that the capture efficiency gap between two immobilization methods narrowed at 30 μg/mg could be well attributed to the k_{on} enhancement of CEA-Ab@MBs at 30 μg/mg.

Supporting Figures and Tables

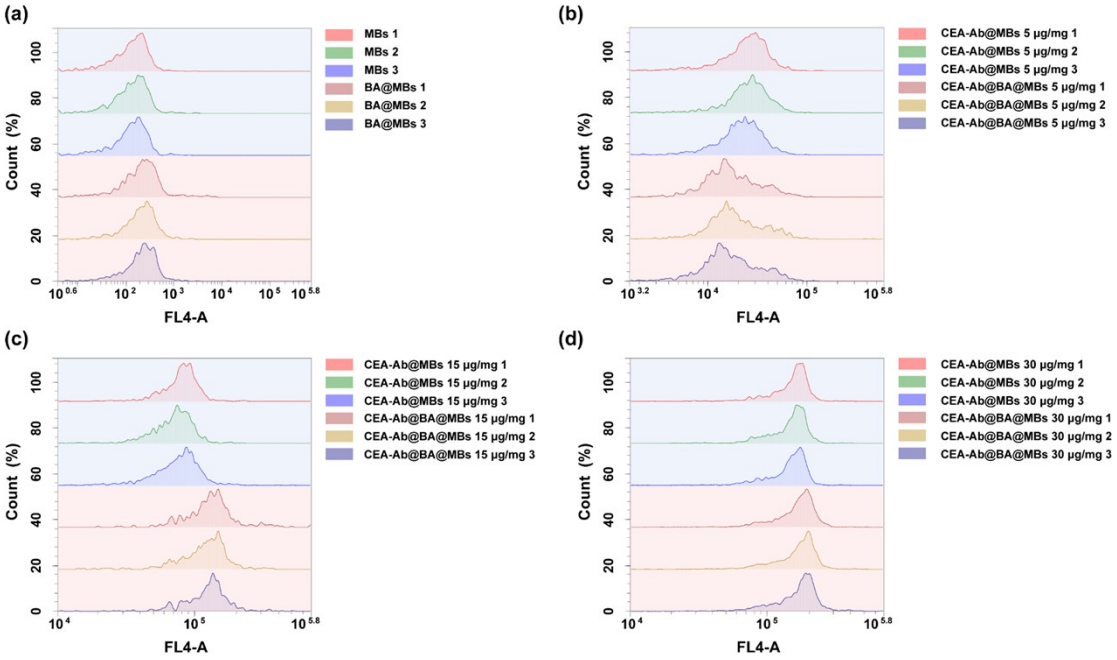

Figure S1. The normalized FSC histograms of anti-F(ab')$_2$ fragments labeled CEA-Ab@MBs and CEA-Ab@BA@MBs in FL4-A channel (*E*x = 640 nm, *E*m = 660±10 nm) at (a) 0 μg/mg, (b) 5 μg/mg, (c) 15 μg/mg, and (d) 30μg/mg antibody density.

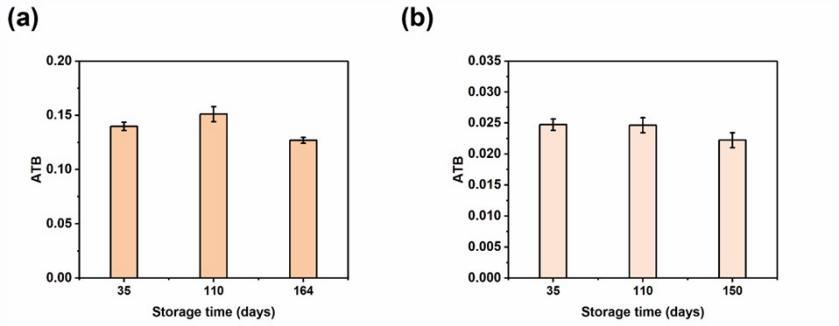

Figure S2. (a) The storage stability of CEA-Ab@BA@MBs characterized by ultra-flow method with 4.95 pg/mL antigen fed. (b) The storage stability of CEA-Ab@MBs characterized by ultra-flow method with 4.95 pg/mL antigen fed.

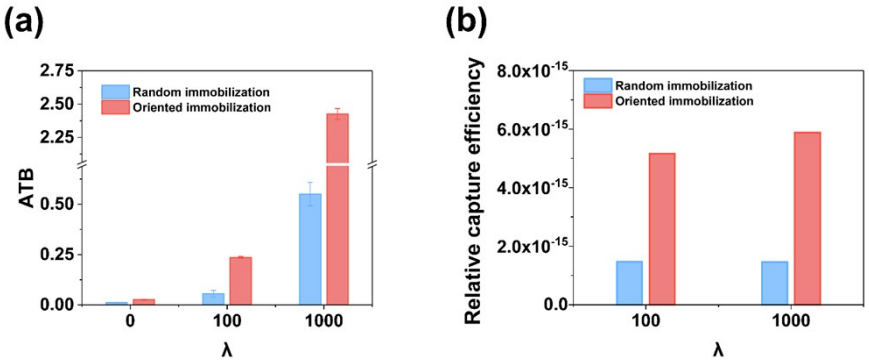

Figure S3. Evaluation of the property of oriented anti-IL4 antibody. (a) ATB of IL4-Ab@BA@MBs and IL4-Ab@MBs with λ equal to 0, 100, 1000 at 30 μg/mg. (b) The relative capture efficiency of IL4-Ab@BA@MBs and IL4-Ab@MBs in digital (λ = 100) and analog (λ = 1000) range at 30 μg/mg antibody concentration.

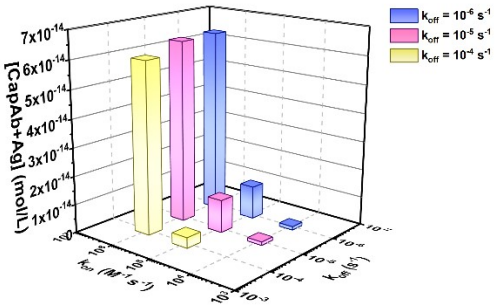

Figure S4. The variation of immunocomplex concentration with the change of k_{on} under different k_{off} at 15 μg/mg under 1 h-incubation. (λ=10) The concentration of immunocomplex was largely influenced by k_{on} rather than k_{off} under the same antibody concentration.

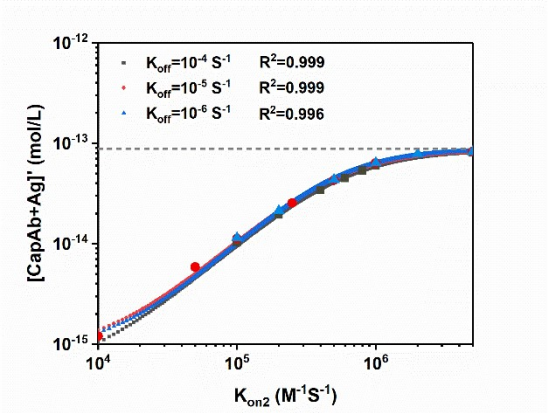

Figure S5. Fitting curve of immunocomplex concentrations of CEA-Ab@BA@MBs as a function of k_{on2} at 15 μg/mg antibody density in 0.5 h. (λ=10)

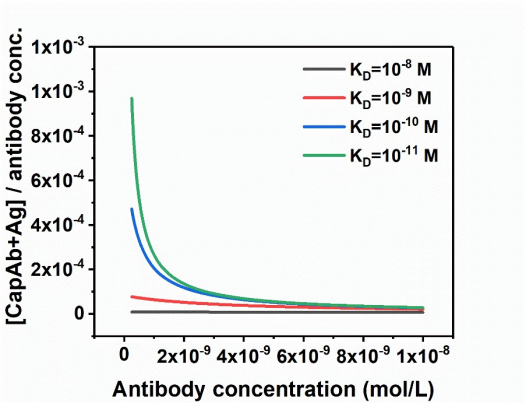

Figure S6. The theoretical relationship between the reaction efficiency unit antibody of the first step and antibody concentration.

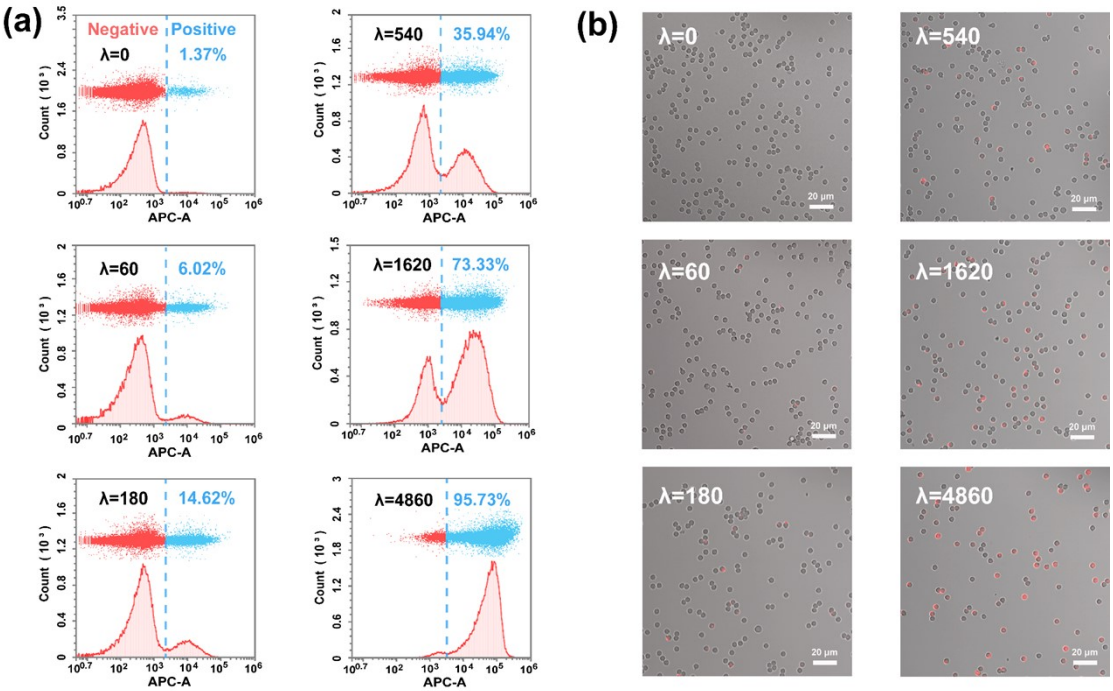

Figure S7. Proof of the CEA-Ab@MBs digital immune response. (a) FSC vs APC-A channel (660 ± 10 nm) scattering plots and counts vs APC-A channel histograms of the CEA-Ab@MBs with λ value from to 0 to 4860. The vertical blue lines represent the threshold that can effectively isolate the positive beads in the control sample as negative ones. (b) Fluorescence images of the CEA-Ab@MBs based immunocomplexes acquired by merging channel 4 (653–700 nm, for Cy5 signal) and bright filed on LSCM with λ value from to 0 to 4860, scale bar, 20 μm.

Table S1. Antibodies and recombinant protein standards used in this work.

Analyte	Capture antibody	Detector antibody	Recombinant protein
CEA	L1C00205 (Hangzhou Biogenome Biotechnology)	L1C00202 (Hangzhou Biogenome Biotechnology)	R040201 (Hangzhou Biogenome Biotechnology)
IL4	500802 (Biolegend)	500702 (Biolegend)	204-IL-010 (R&D Systems)

Table S2. Antibody concentration of all experiments tested by BCA assay.

Antibody type	Antibody concentration (μg/mg)	
	Random immobilization	Oriented immobilization
Anti-human CEA antibody	4.78	5.23
	15.69	14.60
	33.40	31.00
Anti-human IL4 antibody	27.27	30.01

Table S3. Effective antibody amount, antibody number per bead and the occupied area of every antibody.

	Effective antibody amount on 1 mg bead (μg/mg)	Antibody number per bead	Occupied area of every antibody (nm^2)
Oriented Immobilization	5.23	3.56×10^5	79.48
	14.60	9.93×10^5	28.49
	31.00	2.11×10^6	13.41
Random Immobilization	5.99	4.08×10^5	69.32
	8.87	6.03×10^5	46.95
	27.81	1.89×10^6	14.95

Table S4. The immunocomplex concentrations of CEA-Ab@MBs and CEA-Ab@BA@MBs at 1800 s.

k_{off1} (M^{-1} S^{-1})	1.00×10^{-4}		1.00×10^{-5}	
k_{on1} (S^{-1})	1.00×10^4	5.00×10^4	1.00×10^4	5.00×10^4
[CapAb+Ag] (mol/L)	6.77×10^{-16}	3.32×10^{-15}	7.33×10^{-16}	3.60×10^{-15}
[CapAb+Ag]' (mol/L)	9.54×10^{-15}	4.69×10^{-14}	1.03×10^{-14}	5.07×10^{-14}